JOURNAL OF ADVANCED TRANSPORTATION
J. Adv. Transp. 2014; **48**:1017–1029
Published online 15 July 2013 in Wiley Online Library (wileyonlinelibrary.com). DOI: 10.1002/atr.1242

Modelling heavy vehicle car-following behaviour in congested traffic conditions

Kayvan Aghabayk*, Majid Sarvi, Nafiseh Forouzideh and William Young

Institute of Transport Studies, Department of Civil Engineering, Monash University, Victoria, Australia

SUMMARY

This study develops a car-following model in which heavy vehicle behaviour is predicted separately from passenger car. Heavy vehicles have different characteristics and manoeuvrability compared with passenger cars. These differences could create problems in freeway operations and safety under congested traffic conditions (level of service E and F) particularly when there is high proportion of heavy vehicles. With increasing numbers of heavy vehicles in the traffic stream, model estimates of the traffic flow could be degrades because existing car-following models do not differentiate between these vehicles and passenger cars. This study highlighted some of the differences in car-following behaviour of heavy vehicle and passenger drivers and developed a model considering heavy vehicles. In this model, the local linear model tree approach was used to incorporate human perceptual imperfections into a car-following model. Three different real world data sets from a stretch of freeway in USA were used in this study. Two of them were used for the training and testing of the model, and one of them was used for evaluation purpose. The performance of the model was compared with a number of existing car-following models. The results showed that the model, which considers the heavy vehicle type, could predict car-following behaviour of drivers better than the existing models. Copyright © 2013 John Wiley & Sons, Ltd.

KEY WORDS: traffic flow; car-following; truck; heavy vehicles; driving behaviour; congested traffic condition; artificial intelligence; local linear model tree (LOLIMOT); neuro-fuzzy

1. INTRODUCTION

Urban freight movement is a significant and growing proportion of transport movement [1,2]. This increasing growth is likely to be associated with an increase in the proportion of heavy vehicles (HVs) in the traffic stream. Knowledge of the impact of this growth on traffic flow is necessary to ensure correct decisions on the allocation of road space to various road user groups. Microscopic frameworks that capture individual vehicle movements are well-suited to replicating the complexity and uncertainty of the interactions of these user groups on traffic streams. Nevertheless, several major problems including computational performance and the accuracy of models in representing the traffic flow have been reported [3,4].

Car-following and lane changing models form two important underlying components of the traffic microscopic simulations models used to update the dynamic behaviour of vehicles at small discrete intervals. The major limitation of existing microscopic simulation models in representing the integration between various user groups is that they employ a global car-following and lane changing model to capture acceleration characteristics of drivers in all driving situations [5]. However, recent studies have shown the different behaviour of HV drivers during the car-following process

*Correspondence to: Kayvan Aghabayk, Institute of Transport Studies, Department of Civil Engineering, Monash University, Victoria, Australia. E-mail: kayvan.aghabayk@monash.edu

[6,7] and lane changing manoeuvres [8] from those of passenger car (PC) drivers. The heterogeneous traffic flow characteristics and varying road conditions were explored at macroscopic level in details [9–19]. In contrast, the existing microscopic car-following models have not specifically considered the behaviour of HVs. The study reported in this paper is one step in redressing this oversight, in that it develops a model of the following behaviour of HV drivers.

The interaction between PCs and HVs and its influence on traffic flow through the following behaviour of HV drivers is a fundamental component of all network micro-simulation models. This interaction and following behaviour is particularly related to the capacity of freeways when traffic flow is congested [20]. The difficulties of modelling freeway flow breakdown during congested conditions with the existing simulation models are well acknowledged [21]. The traffic flow logic of existing simulation models does not differentiate between the car-following behaviour of PCs and HVs. Microscopic simulations may be capable of modelling freeway sections under low to moderate traffic flows when there are insignificant interactions between vehicles. However, the interactions between the HVs and the surrounding freeway drivers become even more important when traffic flow is close to the capacity. The complex acceleration characteristics of HVs drivers and the significant interactions of the HVs and surrounding vehicles in the adjacent lanes are believed to play an important role in modelling traffic on freeway sections. To address some of the major limitations of the existing microscopic simulation models, this study develops a car-following model for HVs in congested traffic conditions. The model outlined in this paper uses the local linear model tree (LOLIMOT) approach as a powerful artificial intelligence model [22], and a real world data set [23] was used for model calibration and evaluation.

This paper is structured as follows. The next section provides the data analysis, which highlights different following behaviours of HV drivers compared with the PC drivers. This section presents the analysis of space headways, drivers' reaction times and accelerations applied by vehicles during car-following behaviour. This is followed by the model development and model evaluation sections. The paper closes with some conclusions and remarks.

2. DATA ANALYSIS

The Federal Highway Administration (FHWA) has provided trajectory data sets for some of the freeways and arterial roads in California [23,24]. These data sets were created by Cambridge Systematic Incorporation for FHWA as a part of Next Generation Simulation (NGSIM) project. The data analysed in this paper were collected from a segment of Interstate 80 in San Francisco, California on 13 April 2005. Seven video cameras were mounted on the top of a 30-storey building (Pacific Park Plaza) that was located adjacent to the Interstate freeway (I-80). The cameras covered about 503 m of the northbound direction of the freeway.

Trajectory data sets were derived at the resolution of one 10th of second from image processing of the digital videos images for three time slots. The time slots were 4:00–4:15 PM (I-1), 5:00–5:15 PM (I-2) and 5:15–5:30 PM (I-3) all on 13 April 2005. Vehicles have been classified using the FHWA vehicle classification [25] into three different types in the NGSIM data sets: motorcycles, automobiles and HVs. Exhaustive data processing was conducted, and detailed data sets of the vehicle class, size (length and width), two-dimension position, velocity, acceleration and deceleration for all vehicles developed. Each vehicle also has information on the proceeding and following vehicle as well as their lane identification.

The detailed explanation of the study area is presented in FWHA [23]. This includes the traffic characteristics of the site compromising the number of vehicles observed and the traffic flow information during the three time periods. The approach presented in the highway capacity manual [26] was used to determine the level of service (LOS) of the site. The density of each lane was specified during each time slot. It was varied from 36 (fast lane in the first time period, I-1) to 96 (slow lane in the third time slot, I-3) PC per mile. As the Highway Capacity Manual [26] suggested that the density range is between 35 and 45 PC per mile for LOS ‘E’ and greater than 45 for LOS ‘F’, it was concluded that the LOS is ‘E’ and ‘F’. This means that the freeway is operating at capacity or even has more demand than its capacity that can cause a breakdown in vehicular flow.

DOI: 10.1002/atr

A programme written in Microsoft visual studio was used to find HVs and PCs involving in the car-following process. It resulted in finding 204 HVs and 327 PCs in total. These vehicle numbers could generate a considerable number of samples as each car-following process took a few seconds, and because of the data set resolution (1/10 of second), each second produced 10 samples. Table I presents the number of vehicles and the number of samples separately for each time slot.

To highlight different car-following behaviour of HV and PC drivers, three variables were analysed. These variables include headway, acceleration and reaction time, which are discussed in the succeeding text.

2.1. *Headway analysis*

This section analyses the *space headways* in front of HVs and PCs. The space headway was defined as the space gap between two successive vehicles running in the same direction and was calculated from front bumper to front bumper (Figure 1). The headways were extracted from the data set separately for each vehicle type.

The space headways were categorised on the basis of on the speeds of subject vehicles (HVs and PCs) with 5 km/h intervals. The lead vehicle in these cases was PC. Figure 2 shows the average space headways of vehicles at the speed of 0 to 60 km/h. The middle point of each speed interval represents the corresponding speed range. This figure can also show the impacts of the subject vehicle speed on its headway.

The space headways in front of HVs are larger than the corresponding values in front of PCs. Indeed, the distances kept by HV drivers are greater than the distance kept by PC drivers. This different behaviour may be explained by the different braking power-to-mass ratio of HVs and PCs. HVs have a lower power-to-mass ratio than PCs, [27] which results in less reliability and capability of their brakes, and thus, they tend to keep larger space headways when compared with PCs.

The two-sample *t*-test for two independent samples with unknown standard deviation was used to support the aforementioned hypotheses. The null hypothesis was *the space headways in front of heavy vehicles are equal or less than the space headways in front of passenger cars*. The alternative hypothesis, as an alternate to the null hypothesis, would be *the space headways in front of heavy vehicles are greater than space headways in front of passenger cars*. The mean and standard deviation of each speed interval were determined. The hypotheses were tested with 99% level of confidence for each corresponding speed interval of the HV and PC following process. The null hypothesis was

Table I. Number of vehicles and sample sizes.

	I-1		I-2		I-3		Total	
Vehicle type	No. of vehicles	Sample size	No. of vehicles	Sample size	No. of vehicles	Sample size	No. of vehicles	Sample size
Heavy vehicle	90	45 255	68	50 281	46	42 011	204	137 547
Passenger car	153	62 465	102	56 840	72	53 322	327	172 627

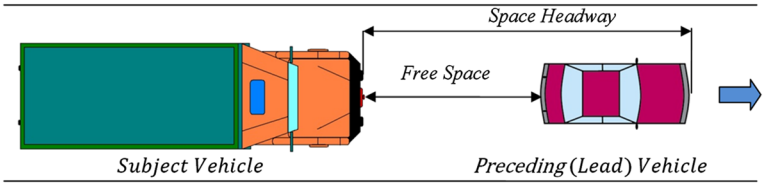

Figure 1. Sketch of car-following.

DOI: 10.1002/atr

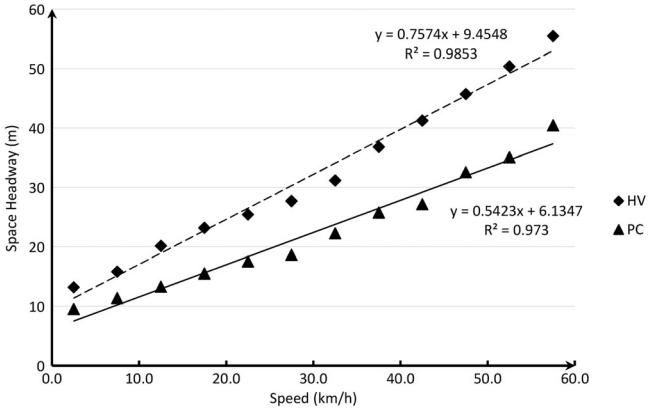

Figure 2. Comparison of space headways in front of heavy vehicles and passenger cars.

rejected with attention to the calculated and critical values of the *t*-statistic presented in Table II. Therefore, the alternative hypothesis was accepted with 99% level of confidence confirming that the space headways in front of HVs are greater than the corresponding values in front of PCs with 99% level of confidence.

2.2. Acceleration analysis

Heavy vehicles have a lower power-to-mass ratio than PCs [27]. The drivers also have better sight distance than PCs because of the height of the cabin. Because of these reasons, it is expected that HV drivers apply lower acceleration than PC drivers. The results of the acceleration analysis are presented here.

The acceleration of the subject vehicle was categorised into 0.1 m/s^2 intervals. The range of the acceleration of the vehicles was between -2 m/s^2 and $+2$ m/s^2. It is noteworthy to mention that this range was smaller when an HV was studied, but the range used in this study was kept similar between HVs and PCs to show the results in the same scale and make the comparison consistent. Further, the outcomes of this section will show the different dispersion of acceleration between HVs and PCs. The number of the acceleration in each type was found, and the proportion was determined as a percentage.

Given the central limit theorem, the real world acceleration distribution of the subject vehicles follows a normal distribution. Figure 3 compares the acceleration distributions of HVs and PCs. The

Table II. The *t*-test results for comparison of space headways.

	Heavy vehicles			Passenger cars			Values of *t*	
Speed range[a]	Sample size	Mean[b]	Standard deviation[b]	Sample size	Mean[b]	Standard deviation[b]	Calculated	Critical
0–5	5197	13.19	7.81	10 137	9.49	4.13	38.41	2.5761
5–10	17 424	15.79	7.62	22 401	11.33	4.84	71.08	2.5760
10–15	19 530	20.13	10.57	23 539	13.26	5.47	86.67	2.5759
15–20	21 642	23.17	13.27	26 223	15.47	7.51	79.74	2.5759
20–25	22 896	25.43	14.94	25 244	17.51	9.69	69.60	2.5759
25–30	18 244	27.69	13.09	22 393	18.63	9.59	80.48	2.5760
30–35	12 135	31.15	16.72	15 882	22.25	12.14	51.60	2.5760
35–40	5965	36.81	23.43	9452	25.73	15.48	35.34	2.5761
40–45	3313	41.23	21.53	4614	27.16	15.86	33.51	2.5764
45–50	2398	45.69	21.95	2756	32.54	16.36	24.57	2.5768
50–55	1708	50.36	19.21	1342	35.05	16.58	23.20	2.5774
55–60	1046	55.46	18.50	470	40.43	17.76	14.82	2.5791

[a]Kilometre per hour.
[b]Metre.

DOI: 10.1002/atr

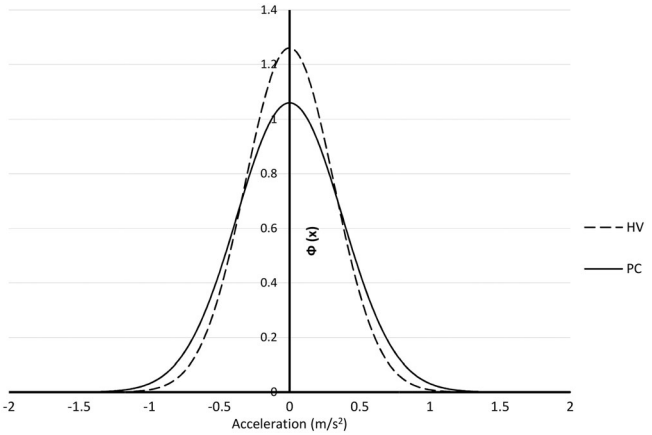

Figure 3. Acceleration distributions of heavy vehicles and passenger cars.

mean and standard deviation in the acceleration distribution of HVs are 0 and 0.316 m/s^2, respectively, whereas these values are 0 and 0.376 m/s^2, respectively, for PCs. Figure 3 shows that the HV distribution is more concentrated than PC distribution. This indicates that HVs apply lower acceleration and follow the leading vehicle in a more smoothing manner compared with PCs.

2.3. Reaction time analysis

The reaction time describes the period between the occurrence or appearance of a stimuli and the driver's reaction. This section investigates the drivers' reaction times influenced by their vehicle types (HV or PC).

The existence of the correlation between the subject vehicle acceleration at time t ($a_n(t)$) and the relative speed between the subject vehicle and its leader at an earlier time, $t-T$, ($\Delta v(t-T)$) was well acknowledged in the literature [28], where T is the driver's reaction time. Indeed, in the car-following process, the reaction can be the acceleration/deceleration of the subject vehicle, and the stimuli can be define as the speed difference between the subject vehicle and its leader. In other words, the subject vehicle driver's reaction can be observed T seconds after the occurrence of a change in the relative speed. This relationship was considered to determine the reaction time of drivers by using Equation (1):

$$a_n(t) \propto \Delta v(t-T) \tag{1}$$

Values of T between 0.5 and 3 seconds were tested. The scatter plots of $a_n(t)$ versus $\Delta v(t-T)$ were derived for various values of T for HVs and PCs. A linear regression was performed for all of the plots, and the strongest correlation between the subject vehicle acceleration, $a_n(t)$, and the relative speed, $\Delta v(t-T)$, was considered as the reaction time [29]. It was found that the reaction times of HV and PC drivers are equal to 1.9 and 1.8 seconds, respectively, which are slightly different.

2.4. Summary

The outcomes of this section showed that the car-following behaviour of HVs differs from that of PCs. Nevertheless, the existing car-following models do not differentiate between PCs and HVs. This points to the need for developing a car-following model in which these different behaviours of HV drivers can be considered. The following section will explain the structure of such a model.

3. MODEL DEVELOPMENT

The LOLIMOT approach [22] can be considered as a new approach to modelling the car-following behaviour of drivers. This model is a locally linear neuro-fuzzy model located in the artificial intelligence

DOI: 10.1002/atr

models category. It offers the opportunity to incorporate human being perceptual imperfections into a rigorous modelling framework. This study predicts the speed of HVs at time t on the basis of the magnitudes of three variables at time $t-T$; where T is the driver's reaction time as determined in Section 2.3. The prediction function can be formulated as follow.

$$V_n(t) = f(V_n(t-T), V_{n-1}(t-T), S(t-T)) \tag{2}$$

In this equation, V_n is the HV speed, V_{n-1} is its leading vehicle speed and S is the free space between them. The free space is considered as the distance between the back bumper of the leading passenger vehicle and front bumper of the HV as shown in Figure 1.

A local linear neuro-fuzzy model is developed and used to solve the car-following problem as a prediction problem. In this structure, each neuron consists of a local linear model (LLM) and an associated validity function which determines the zone of validity of the LLM. Figure 4 shows the structure of such local linear neuro-fuzzy model.

Because each LLM corresponds to a linear model, the outputs of these LLMs can be represented as follows (Equation (3)):

$$\hat{y}_i = w_{i0} + w_{i1}u_1 + w_{i2}u_2 + \ldots + w_{ip}u_p \tag{3}$$

Each $\hat{y}_i$ is a local estimation of the output. In Equation (3), w_{ij} denotes the parameters of the linear model for neuron i, and u_j is the j-th input to the model. In our car-following application, the input vector consists of three elements: $V_n(t-T)$, $V_{n-1}(t-T)$ and $S(t-T)$, which corresponds to u_1, u_2 and u_3, respectively. In this experiment, the size of the input vector p is equal to 3.

Validity functions are defined as normalised Gaussians. Because in this method localities are defined as axis-parallel hyper-rectangles, the validity functions are axis-orthogonal Gaussians, and they have diagonal covariance matrices. These validity functions are defined as follows:

$$\phi_i\left(\underline{u}\right) = \frac{\mu_i\left(\underline{u}\right)}{\sum_{j=1}^{M} \mu_j\left(\underline{u}\right)} \tag{4}$$

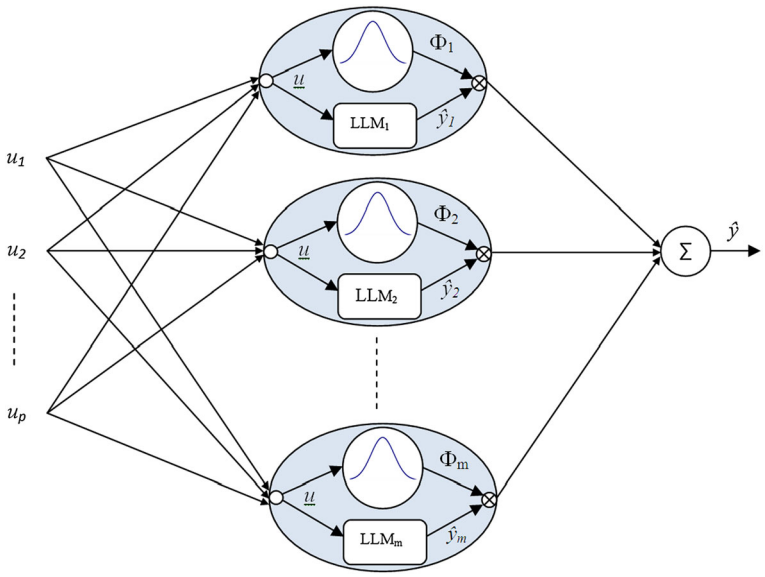

Figure 4. Structure of local linear neuro-fuzzy model.

DOI: 10.1002/atr

Where:

$$\mu_i\left(\underline{u}\right) = \exp\left[-\frac{1}{2}\left(\frac{(u_1 - c_{i1})^2}{\sigma_{i1}^2} + \ldots + \frac{(u_p - c_{ip})^2}{\sigma_{ip}^2}\right)\right] \tag{5}$$

Where c_{ij} denotes the j-th centre coordinate for i-th Gaussian and σ_{ij} denotes the standard deviation in the j-th dimension for the i-th Gaussian. As the validity functions are normalised and they form a partition of unity. For any model input $\underline{u} = \left[u_1\ u_2 \ldots u_p\right]^T$, it can be derived that $\sum_{i=1}^{M} \phi_i\left(\underline{u}\right) = 1$, which allows interpreting each $\phi_i(.)$ as a validity function, because it ensures that the contributions of all local linear models sum up to 1.

The final output of a local linear neuro-fuzzy model $\hat{y}$, which is our estimation of the real output $V_n(t)$, can be computed as follows:

$$\hat{y} = \sum_{i=1}^{M} \hat{y}_i \phi_i\left(\underline{u}\right) \tag{6}$$

Where $\hat{y}_i$ and $\phi_i\left(\underline{u}\right)$ could be computed through Equations (3) and (4), respectively. Thus, the output of local linear models are weighted based on their point dependent validity measure, and the final output is calculated by adding these weighted outputs. It can be said that the network is interpolating between different LLMs with the validity functions.

The required codes were written in MATLAB to predict the speed of the subject vehicle at time t on the basis of three inputs obtained from time $t - T$. Note that, to address the findings of previous section, two different types of subject vehicles were considered in this model including PCs and HVs. The inputs of the model were subject vehicle speed, leading vehicle speed and the free space between the two vehicles all at time $t - T$, and the output was the subject vehicle speed at time t. The I-1 data set was used as the training set for training the structure of the model and adjusting the parameters. The I-3 data set was used as the test set for tuning the model and finding the best structure for the model. The I-2 data set was used as the validation set for evaluating the performance of the learned model. The best structure of the model was found by tracing the errors of the developed model on test data (i.e. I-3), and the model with eight neurons was selected as the best structure, which produces the minimum error. The results showed that new model (LOLIMOT) could provide a good fitness with a high adjusted R-squared ($\overline{R}^2 = 0.93$).

4. MODEL VALIDATION AND EVALUATION

The new model, which was developed via training and testing in the previous section, showed a good performance. However, its performance should be evaluated via another data set that was not used for model development. The basis of this evaluation was to compare the predicted subject vehicle speeds with the corresponding values obtained from real world. Therefore, for each of the samples, the input values (i.e. $V_n(t - T)$, $V_{n-1}(t - T)$ and $S(t - T)$) were given to the model in the form of vector $\underline{u}$, and the model's predicted output $\hat{y}$ is compared with the real output $V_n(t)$ to calculate the error.

The performance of the new model was compared with the performance of two well-known car-following models: neural network-based model and Gipps [30]. Similar to the other existing car-following models, these models do not differentiate between PCs and HVs, and thus, the mixed data were used for calibration and evaluation of the model. The I-1 and I-3 data sets (Table I) were used for model calibration, and the I-2 data set was used for validation and evaluation.

The first model, which was used for evaluation of the new model, was developed based on neural network approach. It used multi-layer perceptron in order to solve the car-following regression problem. Figure 5 shows a typical structure of the model. The model had three inputs and one output.

DOI: 10.1002/atr

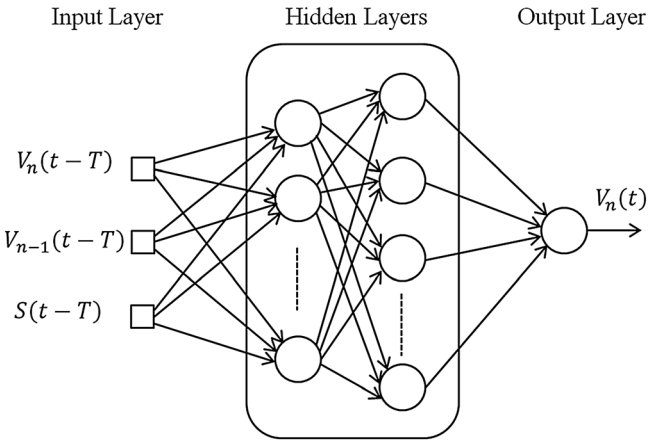

Figure 5. A typical structure of the neural network model.

The inputs of the model were the subject vehicle speed, the leading vehicle speed and free space between the subject vehicle and its leader all at time $t-T$. These variables were used to predict the speed of subject vehicle at time t.

The structure of the model consists of several layers, each of which has a number of neurons. Each neuron generates a nonlinear output on the basis of a sigmoidal transfer function. The input of each neuron is a linear combination of the previous layer outputs. In this study, the back-propagation approach as a well-known training algorithm was used for learning of the network parameters. Several structures were investigated, and the network with minimum average error on test data was used for comparison.

The Gipps [30] car-following model was the second model, which was used for evaluation purpose. This model is widely used in micro-simulations such as AIMSUN [31]. Gipps [30] car-following model considers two constrains to estimate the subject vehicle speed as provided in Equation (7).

$$v_n(t+T) = Min \begin{cases} v_n(t) + 2.5a_nT(1 - v_n(t)/V_n)\left(0.025 + v_n(t)/{V_n}^d\right)^{1/2} \\ b_n + \left\{ b_n^2T^2 - b_n\left[2(x_{n-1}(t) - L_{n-1} - d_{n-1} - x_n(t)) - v_n(t)T - \frac{v_{n-1}^2(t)}{b'}\right\}^{0.5} \end{cases} \quad (7)$$

where: a_n is the maximum acceleration that the driver of vehicle n wishes to undertake;
b_n is the most severe braking that the driver of vehicle n wishes to undertake ($b_n < 0$);
L_{n-1} is the physical length of the vehicle;
d_{n-1} is the margin into which the following vehicle is not willing to intrude, even when at rest;
${V_n}^d$ is the desired speed or the speed at which the driver of vehicle n wishes to travel;
$x_n(t)$ is the location of the front of vehicle n at time t;
$v_n(t)$ is the speed of vehicle n at time t;
b' is the estimation of b_{n-1} employed by the driver of vehicle n; and
T is drivers' reaction time

A genetic algorithm was used to calibrate the model findings a_n, b_n, d_{n-1} and b'. The objective function presented in Equation (8) was minimised by the implementation of genetic algorithm considering the constrain found in Rakha *et al*., [32] regarding to b/b'.

$$MSE = \frac{\sum_{i=1}^{N}[V(estimated) - V(real)]^2}{N} \quad (8)$$

DOI: 10.1002/atr

Figures 6 and 7 show a typical speed diagram of a PC and an HV, respectively. These vehicles have been randomly selected amongst the vehicles during car-following process from the I-2 data set. They show the real world and predicted speeds of the vehicles obtained from the outputs of the LOLIMOT, neural network and Gipps [30] car-following models to provide a visual comparison of the models. As it can be seen, the new model can fit the real world data better compared with the existing models.

Table III compares the performance of the two aforementioned car-following models on the evaluation data set (I-2). The results showed that the new model that can differentiate subject vehicle type could predict the following process better than the neural network and Gipps [30] car-following models. The adjusted R-squared $\left(\overline{R}^2\right)$ of the LOLIMOT is 0.92, and the corresponding values are 0.84 and 0.63 for neural network and Gipps [30], respectively. The error of new model was also less than

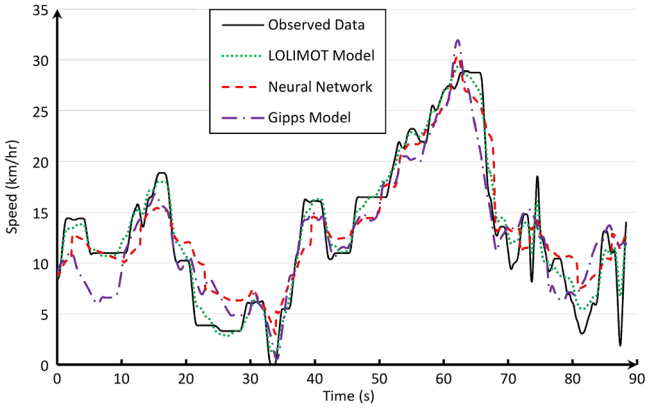

Figure 6. A typical speed diagram of a passenger car.

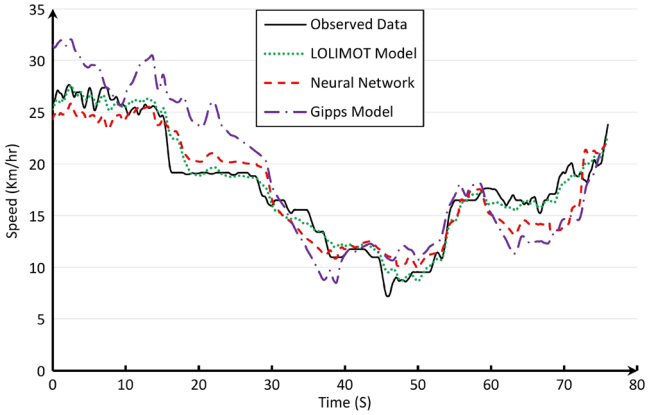

Figure 7. A typical speed diagram of a heavy vehicle.

Table III. Comparison of model performances.

			LOLIMOT		
	Gipps [30]	Neural Network	PC	HV	Total
R^2	0.63	0.84	0.91	0.94	0.92
RMSE	7.04	4.53	3.22	2.95	3.10

LOLIMOT, local linear model tree; PC, passenger vehicle; HV, heavy vehicle; RMSE, root mean squared error.

DOI: 10.1002/atr

the existing model. The root mean squared error of the LOLIMOT is 3.10 km/hour. However, the corresponding values for the neural network and Gipps [30] are 4.53 and 7.04 km/hour, respectively. Table III also provides the performance results of the new model prediction separately on the basis of the subject vehicle types. In summary, the new model distinguishes between HVs and PCs and provides higher $\overline{R}^2$ and lower root mean squared error indicating its better fitness compared with the existing models.

There are some reasons that could explain the better performance of the new model. The most important one is considering different vehicle types and then using local approach rather than applying a global method. Modelling the behaviour of a driver depends on a variety of factors, and this modelling differs from one situation to another. Therefore, a local approach that divides the global space into some regions could achieve a better performance compared with the models that use the whole space for modelling. The neural network and Gipps [30] car-following models use a global method to predict driver's behaviour. In fact, the parameters of the models have a global effect and are used to predict all situations and cases. However, the new model not only differentiates between PCs and HVs for parameter adjustments but also uses several local models to consider different situations. More precisely, by hierarchical division of the space, this model is able to increase the resolution in regions. This leads to the construction of an adaptive model that can model dissimilar situations differently, and consequently, it can precisely fit to the data. Adaptive resolution partitioning is a robust idea when dealing with problems where distribution of samples varies in different regions. For example, the method can keep the resolution low where the samples are sparse. Further, it can increase the resolution in denser areas and regions that is hard to predict because of nonlinearity or uncertainty. The main concern in training such as a machine learning method is to avoid over-fitting, which has been overwhelmed by using the test data for assessment of the learned model in this study.

Another reason for the good performance of the new model is the consideration of uncertainty of human's perceptions while following another vehicle. The new model uses fuzzy approach to aggregate the linear models, which makes it capable to handle uncertainties.

In fact, the new model could predict the car-following behaviour of HV and PC drivers separately with high precision by differentiating between the subject vehicle types and using the fuzziness property and the local approach.

5. CONCLUSION

This paper highlighted some of the different behaviour of HV drivers while following another vehicle and compares with that of PC drivers. It was shown that HV drivers tend to keep larger headway to the front vehicles, apply a lower acceleration and follows a preceding vehicle with less speed changes (smoother) than PC drivers. Further, the reaction time of drivers varies slightly according to their vehicle types.

This study developed a new car-following model that specifically considered HV. The model used the LOLIMOT approach to predict the following (subject) vehicle speed with consideration of the vehicle type. Three different time slots of a data set obtained from a stretch of a freeway in USA were used in this study; two of them for training and testing purpose and another one for evaluating the proposed model.

The performance of the new model was evaluated by comparison of the results obtained from the model with the outcomes of two existing car-following models. Gipps [30] car-following model and a neural network-based car-following model were used for this purpose. Note that these models similar the other existing models do not differentiate between HV and PCs. The results showed that the new model can fit the real world driver's car-following behaviour better compared with the existing models. It was shown that the adjusted R-squared $\left(\overline{R}^2\right)$ of the proposed model was considerably higher than the corresponding values of the existing models. Further, the comparison between the real world and predicted data showed that the error of the LOLIMOT model was much less than the existing models. The error of the Gipps [30] car-following model was 2.3 times greater than the proposed model error. This ratio was about 1.5 for the neural network model.

DOI: 10.1002/atr

The new model could incorporate the different car-following behaviour of HVs and PCs. The next step of this work includes implementation of the developed model to a micro-simulation to quantify the effect of the developed model using variety of traffic scenarios. This work could be of notable interest for researchers attempting to replicate HV behaviour in micro-simulation models.

6. LIST OF ABBREVIATIONS AND SYMBOLS

LOLIMOT	Local Linear Model Tree
BTRE	Bureau of Transport and Regional Economics
FHWA	The Federal Highway Administration
NGSIM	Next Generation Simulation project
HCM	Highway Capacity Manual
LOS	Level of Service
HV	Heavy Vehicle
PC	Passenger Car
No.	Number
km/h	kilometre per hour
m	metre
R^2	the coefficient of determination denoted R^2 and pronounced R squared
$\overline{R}^2$	adjusted R squared
m/s^2	metre per second squared (the unit of acceleration in the International System of Units)
t	an index denoting a time step
$a_n(t)$	the acceleration/deceleration of the subject vehicle n at time t
T	the driver's reaction time (seconds)
$\Delta v(t-T)$	the relative speed between the subject vehicle and its leader at an earlier time, t-T
$\propto$	the symbol represents "is proportional to"
f	prediction function
$V_n(t)$	the speed of the subject vehicle n at time t
$V_n(t-T)$	the speed of the subject vehicle n at an earlier time, t-T
$V_{n-1}(t-T)$	the leading vehicle speed at an earlier time, t-T
$S(t-T)$	the free space between the subject vehicle and the leading vehicle at an earlier time, t-T
LLM	Local Linear Model
$\hat{y}_i$	the output of the i-th LLM in the LOLIMOT which is a local estimation of the real output
w_{ij}	the parameters of the linear model for neuron i
$\underline{u}$	transpose of vector u which is the input vector to the proposed model
u_j	the j -th element of the input vector to the proposed model
p	the number of elements in the input vector of the proposed model
u_1	the element of the input vector to the model which represents $V_n(t-T)$
u_2	the element of the input vector to the model which represents $V_{n-1}(t-T)$
u_3	the element of the input vector to the model which represents $S(t-T)$
ϕ_i	the validity function of the i-th locality in the LOLIMOT which is a normalized Gaussian
μ_i	The Gaussain function of the i-th validity function
c_{ij}	the j -th center coordinate for i -th Gaussian (validity function) of the LOLIMOT
σ_{ij}	the standard deviation in the j -th dimension for the i -th validity function of the LOLIMOT
$\hat{y}$	the final output of the model which is the estimation of the real output, subject vehicle speed at time t $V_n(t)$
M	the number of localities in the LOLIMOT
$exp()$	exponential function
MLP	Multi-Layer Perceptron neural network

DOI: 10.1002/atr

a_n	the maximum acceleration which the driver of vehicle n wishes to undertake (Gipps model parameter)
b_n	the most sever braking that the driver of vehicle n wishes to undertake ($b_n < 0$, Gipps model parameter)
L_{n-1}	the physical length of the leading vehicle in the Gipps model
d_{n-1}	the margin into which the following vehicle is not willing to intrude, even when at rest (Gipps model parameter)
V_n^d	the desired speed or the speed at which the driver of vehicle n wishes to travel in the Gipps model
$x_n(t)$	the location of the front of vehicle n at time t in the Gipps model
$v_n(t)$	the speed of vehicle n at time t in the Gipps model
b'	the estimation of b_{n-1} employed by the driver of vehicle n (Gipps model parameter)
MSE	Mean Squared Error
RMSE	Root Mean Squared Error

REFERENCES

1. BTRE. Urban pollutant emissions from motor vehicles: Australian trends to 2020. Bureau of Transport and Regional Economics, Department of Transport and Regional services, Report for Environment Australia, 2003.
2. Wright SJ. Review of urban congestion trends, impacts and solutions (Consultancy Report). *Traffic Management Systems for Australian Urban Freeways*, Prepared by ARRB Consulting for Council of Australian Governments: Canberra, 2006.
3. Robinson S. Discrete-event simulation: from the pioneers to the present, what next? *Journal of the Operational Research Society* 2004; **56**(6):619–629.
4. Alexiadis V, Jeannotte K, Chandra A. Traffic Analysis Tools Primer, prepared for US DOT/FHWA, Oakland, CA: Cambridge Systematics, 2004.
5. Panwai S, Dia H. Comparative evaluation of microscopic car-following behavior. *IEEE Transaction on intelligent transportation systems* 2005; **6**(3):314–325
6. Aghabayk K, Sarvi M, Young W. Understanding the dynamics of heavy vehicle interactions in car-following. *Journal of Transportation Engineering* 2012; **138**(12):1468–1475
7. Sarvi M. Heavy commercial vehicles following behaviour and interactions with different vehicle classes. *Journal of Advanced Transportation* 2011; DOI: 10.1002/atr.182.
8. Aghabayk K, Moridpour S, Young W, Wang, Y, Sarvi M. Comparing Heavy Vehicle and Passenger Car Lane Changing Manoeuvres on Arterial Roads and Freeways. *Transportation Research Record, Journal of the Transportation Research Board.* 2011; **2260**(1):94–101.
9. Wong GCK, Wong SC. A multi-class traffic flow model - an extension of LWR model with heterogeneous drivers. *Transportation Research Part A* 2002; **36**:827–841.
10. Gupta AK, Katiyar VK. A new multi-class continuum model for traffic flow. *Transportmetrica* 2007; **3**:73–8.
11. Ngoduy D, Hoogendoorn SP, Liu R. Continuum modeling of cooperative traffic flow dynamics. *Physica A* 2009; **388**:2705–2716.
12. Tang TQ, Huang HJ, Shang HY, Zhao SG. A new dynamic model for heterogeneous traffic flow. *Physics Letters A* 2009; **373**:2461–2466.
13. Tang TQ, Huang HJ, Shang HY. A dynamic model for the heterogeneous traffic flow consisting of car, bicycle and pedestrian. *International Journal of Modern Physics C* 2010; **21**:159–176.
14. Tang TQ, Huang HJ, Shang HY. A macro model for bicycle flow and pedestrian flow with the consideration of the honk effects. *International Journal of Modern Physics B* 2011a; **25**(32):4471–4479.
15. Bellomo N, Bellouquid A. On the modelling of vehicular traffic and crowds by the kinetic theory of active particles. In *Mathematical Modelling of Collective Behaviour in Socio-ecomonics and Life Sciences*, Naldi G, Pareschi L and Toscani G (eds). Birkhäuser: Boston, 2010; 273–296.
16. Zhang P, Wong SC, Dai SQ. A note on the weighted essentially non-oscillatory numerical scheme for a multi-class Lighthill-Whitham-Richards traffic flow model. *Communication in Numerical Methods in Engineering* 2011; **25**:1120–1126.
17. Li CY, Tang TQ, Huang HJ, Shang HY. A new car-following model with consideration of driving resistance. *Chinese Physics Letters* 2011; **28**:038902.
18. Tang TQ, Caccetta L, Wu YH, Huang HJ, Yang XB. A macro model for traffic flow on road networks with varying road conditions. *Journal of Advanced Transportation* 2011b; DOI: 10.1002/atr.215
19. Tang TQ, Wang YP, Yang XB, Wu YH. A new car-following model accounting for varying road condition. *Nonlinear Dynamics* 2012; **70**:1397–1405.
20. Sarvi M, Kuwahara M, Ceder A. Observing freeway ramp merging phenomena in congested traffic. *Journal of Advanced Transportation* 2007; **41**(2):145–170
21. Hidas P. A functional evaluation of microsimulation models, CAITER conference, Melbourne, Australia, 2004.

22. Nelles O. *Nonlinear System Identification: From Classical Approaches to Neural Networks and Fuzzy Models*. Springer Verlag: Berlin, 2001.
23. FHWA. NGSIM data set. Freeway data set. Federal Highway Administration. 2005. URL http://ngsim-community.org/.
24. FHWA. NGSIM data set. Arterial data set. Federal Highway Administration. 2006. URL http://ngsim-community.org/.
25. FHWA. Vehicle classification. Federal Highway Administration. 2010. URL http://www.fhwa.dot.gov/policy/ohpi/vehclass.htm [access on 2010].
26. HCM. *Highway Capacity Manual*. TRB, National Research Council: Washington, D.C., 2010.
27. Ramsay ED. Interaction of multi-combination vehicles with the urban traffic environment. *5th International Symposium on Heavy Vehicle Weights and Dimensions*, Maroochydore, Queensland, 1998, 151–167.
28. Brackstone M, McDonald M. Car-following: a historical review. *Transportation Research Part F* 1999; **2**(4):181–196.
29. Sarvi M. Freeway weaving phenomena observed during congested traffic. *Transportmetrica A: Transport Science* 2013; **9**(4):299–315.
30. Gipps PG. A behavioural car following model for computer simulation. *Transportation Research B* 1981; **15**(2):105–111.
31. AIMSUN. Aimus 7 users' manual. *Transport Simulation System (TSS), Barcelona, Spain*, 2011.
32. Rakha H, Pecker C, Cybis H, Beatriz B. Calibration procedure for Gipps car-following model. *Transportation Research Record: Journal of the Transportation Research Board* 2007; **1999**(1):115–127

DOI: 10.1002/atr